JOURNAL OF INTENSE PULSED LASER AND APPLICATIONS IN ADVANCED PHYSICS Vol. 1, No. 1, 2011, p. 13 – 20

New functional materials designed by laser based technology

N. TOMOZEIU
R&D Department, Océ Technologies B.V., P.O. Box 101, 5900 MA Venlo, The Netherlands

The complete integration of silicon based optoelectronic devices is suffering for many decades because silicon is an inefficient emitter of light. Low-dimensional silicon systems as porous silicon, super-lattices of Si/SiO_2, silicon nano-pillars, silicon nanocrystals embedded in SiO_2 or in Si_3N_4 are considered by specialists as possible solutions to produce a silicon based laser-diode. Pavesi at al have observed modal and net optical gains in silicon nanocrystals (Si-nc) embedded in an insulator matrix. It was found that the photoluminescence (PL) properties are influenced by the size of the nano-crystals and by the interface with the matrix material. However, the route towards the realization of a silicon-based laser, and from here, of a highly integrated silicon based optoelectronic chip is open. The Si-nc embedded in a SiO_2 matrix is preferable because of the compatibility between Si and SiO_2 and, why not, because of the huge experience in nano- and micro-electronics technology. In order to obtain the Si-nc structures in SiO_2, techniques as implantation of silicon ions in SiO_2 layer, followed by thermal annealing, or using silicon sub-oxides SiO_x ($0<x<2$) as precursors, and annealing and/or ion bombardment have been reported. The post deposition treatment enhances the phase separation processes resulting in silicon islands dispersed in a SiO_2 material. Herewith we propose another post deposition technique based on UV laser irradiation of the SiO_x thin films. It is known that the irradiation with energetic photons changes the structure of amorphous materials (carbon nitride or amorphous silicon). In this paper, are summarised the main results of our researches on laser UV photons interacting with SiO_x material.

(Received March 05, 2011; accepted March 23, 2011)

Keywords: SiO_2, Functional materials, UV photons

1. Introduction

Silicon based nano- / micro-electronics have been missed for many decades the complete integration within an optoelectronic device because the silicon is an inefficient emitter of light. Being a semiconductor with an indirect bandgap and having efficient free carrier absorption of the radiation, the crystalline silicon was considered an inadequate material for laser diodes to produce totally integrated optoelectronic devices. In the last two decades, a special attention has been paid to light-emission properties of low-dimensional silicon systems: porous silicon[1,2], super-lattices of Si/SiO_2 [3], silicon nano-pillars[4], silicon nanocrystals embedded in SiO_2 [5] or in Si_3N_4 [6]. Both, the theoretical understanding of the physical mechanisms (quantum confinement of excitons in a nano-scale crystalline structure) and the technological advance to manufacture such structures have contributed to produce a silicon based laser.

Pavesi at al [7] have been unambiguously observed modal and net optical gains in silicon nanocrystals. They have compared the gain cross-section per silicon nano-crystal with that one obtained with A_3B_5 quantum dots and it was found orders of magnitude lower. However, owing to the much higher stacking density of silicon nanocrystals with respect to direct-bandgap A_3B_5 quantum dots, similar values for the material gain are observed. In this way, the route towards the realization of a silicon-based laser, and from here, of a highly integrated silicon based optoelectronic chip, is open.

The silicon nano-crystals (Si-nc) embedded in various insulators matrix have been intensively studied in the last decade. Either the photoluminescence (PL) properties of the material or the emitted radiation from a LED/ diode laser structure was studied. A clear statement was made: the peak position of PL blueshifts with decreasing the size of Si-nc. The nano-crystals interface with the matrix material has a great influence on the emission mechanism. It was reported that due to silicon-oxygen double bonds, Si-nc in SiO_2 matrix has localised levels in the band gap and emits light in the near-infrared range of 700–900 nm even when the size of Si-nc was controlled to below 2 nm

[1] A.G. Cullis and L.T. Canham, *Nature* **353** (1991) 335
[2] M.V. Wolkin, J. Jorne, P.M. Fauchet, G. Allan and C. Delerue, *Phys. Rev. Lett*. **82**, (1999) 197
[3] Z.H Lu, D.J. Lockwood and J.M. Baribeau, *Nature* **378** (1995) 258
[4] A.G. Nassiopoulos, S. Grigoropoulos and D. Papadimitriou, Appl. Phys. Lett. **69** (1996) 2267
[5] W.L. Wilson, P.F. Szajowski and L.E. Brus, *Science* **262**, (1993) 1242
[6] K.S. Cho, N-M. Park, T-Y. Kim, K-H. Kim, G. Y. Sung and J. H. Shin, Appl. Phys. Lett. **86** (2005) 071909
[7] L. Pavesi, L. Dal Negro, C. Mazzoleni, G. Franzo and F. Priolo, *Nature* **408** (2000) 440

[2, 8]. Pavesi at al[7] have proposed a three levels model to explain the experimental data: two levels correspond to the lowest unoccupied molecular orbital (LUMO) and to the highest occupied molecular orbital (HOMO), and the third level is due to the radiative interface state. With other words, they have introduced the bottom of the conduction band, the top of the valence band of the nano-crystal, respectively, and a localised level in the bandgap region (see the figure 7 from [7]). By optical excitation, the LUMO is populated emptying the HOMO level. These electrons on excited state relax very rapidly to the interface states. The stimulated emission happened when the electrons from the interface states recombine the holes from the valence band. Therefore, the interface between the Si-nc and the SiO_2 (insulator matrix) is very important. The density and the energy of the interface states are dependent on the deposition mechanism and post deposition treatment of the dielectric material with embedded nano-crystals.

Many papers have been dedicated to physical properties of thin films of Si-nc structures in a SiO_2 matrix obtained by implantation of silicon ions, followed by thermal annealing[7,9,10]. However, such structures can be obtained from silicon sub-oxides SiO_x ($0<x<2$) as predecessors, and annealing[11] and/or ion bombardment[12]. The post deposition treatment enhanced the phase separation processes, and from a homogeneous SiO_x layer a new material with silicon islands dispersed in a SiO_2 sea is formed. Besides annealing and ion bombardment, another post deposition technique based on laser irradiation of the SiO_x thin films have been proposed[13] to study the spinodal decomposition as a phase separation process[14]. The irradiation with energetic photons changes the structure of the amorphous materials. Ultraviolet (UV) light has been used to induce structural modification in amorphous carbon nitride[15] or amorphous silicon[16]. In this paper, are summarised the main results on the laser photon interaction with the SiO_x materials with the final purpose to obtain Si-nc entities into a SiO_2 matrix. Therefore, irradiating amorphous silicon suboxides with laser UV photons, one can produce silicon nano-crystals for photons emitters from silicon.

2. On the SiO_x structure

Structural changes can be induced by energy transfer into any type of material if the delivered energy amounts the value to breaking the inter-atomic bonds. In order to estimate the needed energy to break all bonds in a unity volume of SiO_x, a very simple model can be utilized. The Si – Si and Si – O bonds are characterised by a dissociation energy of 3.29 eV/bond and 8.26 eV/bond, respectively[17]. The particles' density in c-Si is $5 \cdot 10^{28}$ m^{-3} while for c-SiO_2 is $6.72 \cdot 10^{28}$ m^{-3}. Interpolating, it can be found for SiO_x:

$$N_{SiO_x}^{at} = 5 \cdot 10^{28} + 8.55 \cdot 10^{27} \cdot x \quad (m^{-3}), \tag{1}$$

where x=O/Si.

The silicon atoms' density is:

$$N_{Si} = N_{SiO_x}^{at} \cdot \frac{1}{1+x} \tag{2a}$$

and the oxygen atoms' density is:

$$N_O = N_{SiO_x}^{at} \cdot \frac{x}{1+x} \; . \tag{2b}$$

Taking into account the fact that the silicon atom is four-coordinated and the oxygen is two-coordinated, the number of bonds can be easily calculated, considering that:

i) O atoms will participate at Si – O – Si bridges, which mean two Si-O bonds:

$$n(Si-O-Si) = 2 \cdot n(Si-O) = N_O, \tag{3a}$$

(we note that n(X-Y) is the number of bonds between X and Y atoms, and N_Y is the number of Y atoms),

ii) Si atoms will contribute at Si – Si and Si – O – Si bonds:

$$n(Si-Si, Si-O-Si) = (4/2) \cdot N_{Si} \, .$$

This means that for Si – Si bonds it is easy to write:

$$n(Si-Si) = \frac{4}{2} N_{Si} - N_O = N_{SiO_x}^{at} \cdot \frac{2-x}{1+x}. \tag{3b}$$

Having the number of bonds and the energy per bond, the necessary energy in order to break all bonds can be estimated. In Fig. 1 (a) it is shown the density of Si – Si

[8] A. Puzder, A. J. Williamson, J. C. Crossman, and G. Galli, Phys. Rev. Lett. **88** (2002) 097401
[9] N. Lalic and J. Linnros, J. Lumin. **80** (1999) 263
[10] P. J. Walters, G. I. Bourianoff and H. A. Atwater, Nat. Mater. **4** (2005) 143
[11] B.J. Hinds et al – Mat. Res. Soc. Symp. Proc. Vol. 452 (1997) 452
[12] A. Milela, M. Creatore, M. C. M. v/d Sanden and N. Tomozeiu, J. Optoelectronics and Advanced Materials, Vol. **8**, No. 6 (2006) 2003
[13] N. Tomozeiu, Applied Surface Science **253** (2006) 376–380
[14] J. J. van Hapert, A. M. Vredenberg, E. E. van Faassen, N. Tomozeiu, W. M. Arnoldbik, and F. H. P. M. Habraken, Physical Review B **69**, (2004) 245202
[15] M. Zhang and Y. Nakayama, J. Appl. Phys. 82 (10) (1997) 4912.
[16] G. Aichmayr, D. Toet, M. Mulato, P.V. Santos, A. Spangenberg, S. Christiansen, M. Albrecht and H.P. Strunk, Phys. Status Solidi A166 (1998) 659.
[17] *Handbook of Chemistry and Physics* , the 48-th edition, The Chemical Rubber Publishing Co. (1968) F149

and Si – O bonds versus composition (x parameter from SiO_x) while in Fig. 1 (b) are given the energy values (in J/ m^3) calculated for x ranging between 0 and 2. For a sample with certain composition (x value), if the corresponding value of the dissociation energy is instantaneously delivered, we can consider that for an extremely short time, the bonds are broken and the atoms can "look for" more stable configurations. With short laser pulses, such kind of experiments can be made and structural changes of the material can be studied.

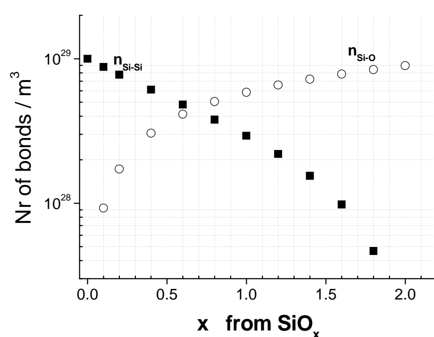

(a)

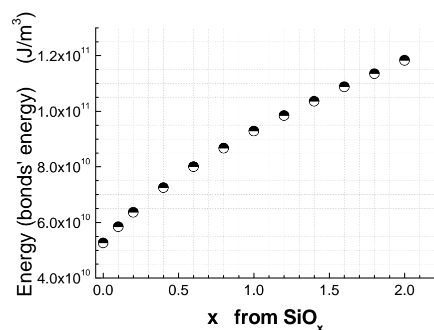

(b)

Fig. 1. (a) The calculated values of the Si-Si and Si-O bonds density as a function of x - the oxygen content; (b) The dissociation energy per volume unit versus x parameter.

Within a disordered material, the structural defects are often part of the structure. The calculations shown in this section did not consider these defects. However, the defects' density is a very important parameter for thin films of silicon suboxide. The defect types and density will define the electrical parameters of the layers[18]. If their density is big enough they can also influence the structural properties. The most frequent defect type in amorphous semiconductors is the *dangling bond* (DB) defect. If the electron associated to this bond remains attached to its atom, the defect is neutral (D^0). In many situations this electron will electrically interact with neighbours: i) and it can get another electron forming a pair spin coupled electrons, or ii) the electron will leave the dangling bond for a position more favourable. In the first case, the defect will become negatively charged (D^-, it has an extra electron) while in the second case de defect will be positively charged (D^+) because it losses one electron. Investigating the energy associated to and the density of the defects are important tasks. The neutral defects are paramagnetic and they can be detected by Electron Paramagnetic Resonance (EPR).

3. Experimental

3.1 Sample preparation

Thin films of a-SiO_x have been deposited in a reactive 13.56 MHz r.f. magnetron sputtering system. Using argon plasma, silicon atoms are sputtered from a polycrystalline silicon target. Keeping constant the r.f. power (2.2 kW) and the argon pressure (0.3 Pa) various SiO_x compositions are obtained by adding O_2 to the sputtering gas. During depositions, the plasma has been monitored by optical emission spectroscopy. No notable intensity variations of the emitted light assigned to silicon and oxygen atoms have been measured during a deposition. This suggests a homogeneous deposited layer thickness. Samples with a thickness of 330 nm have been deposited onto c-Si substrates.

The substrate was not heated externally, but immediately after deposition, the layer temperature was found lower than 100^0C.

For the research here presented, the experiments have been made on samples with oxygen contain defined by x=1.2. The layer composition has been determined by Rutherford back-scattering (RBS) and energy recoil detection (ERD) analysis. The results fit very well, and they are x=1.21 for RBS and x=1.22 for ERD.

Structural and compositional changes of SiO_x samples with different oxygen content have been observed when the SiO_x layers had been bombarded with energetic ions [19]. For this work the samples have been irradiated, in a controllable way, with UV photons.

3.2 SiO_x laser treatment

After deposition the samples have been kept in normal atmosphere conditions. They were irradiated with a laser UV light (λ=248 nm) of various energy in a argon atmosphere. A pulsed KrF laser has been utilized and the irradiation was made with a frequency of 50 Hz. Each pulse had a length of 20 ns. A surface of 2.6 x 10 mm^2 was irradiated with energies between 0 and 71 mJ/shot.

The absorbance spectra of the laser photons have been measured using a Perkin Elmer UV-VIS system. Utilising

[18] F. Iacona, G. Franzo and C. Spinella, J. of Appl. Physics vol 87, nr 3, 1295 (2000)

[19] W.M. Arnoldbik, N. Tomozeiu, F.H.P.M. Habraken, Vacuum 73 (2004) 109

the versatility of the Scout program[20] to model the depth profile of this absorbance, the percentage of the incident light, which was absorbed, was estimated. In figure 2 the depth profile of the absorbance is presented. It is easy to observe that the absorbance vanishes in $SiO_{1.2}$ after 130 nm. As a result, we conclude that 84.9 % from the incident energy is absorbed in $SiO_{1.2}$. The rest of the photons is lost by reflection. We mention that experimentally we have found this amount being dependent on the oxygen content in the sample: silicon rich samples absorb at the very surface - small depth of penetration - while, for the oxygen rich samples the photon depth penetration is larger and the absorbed energy is higher (data not shown here).

The incident laser energy, E, is calculable measuring the energy per shot and knowing the number of shots. The surface energy density, σ, defined as the total laser energy divided by the irradiated area, was also calculated. For the experimental arrangement utilized in these studies, the correlation factor between the incident energy and surface energy density was: $\sigma\left(\mathrm{mJ/mm^2}\right) = 1.88 \cdot \mathrm{E}\left(\mathrm{mJ}\right)$.

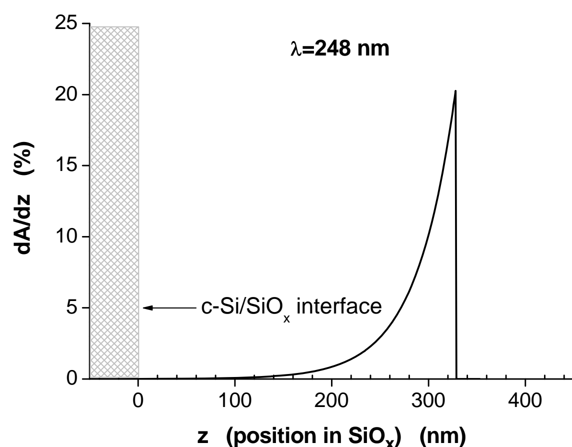

Fig. 2. The variation of the optical absorbance of photons with λ=248 nm in $SiO_{1.2}$ layers. The light was incident on the samples under an incidence angle of 10^0.

One has to be noted that the pulse duration was 20 ns and the time between two successive pulses was 20 ms. Therefore, the most part of a cycle, the sample was non-irradiated. In experiments of ion beam bombardment on a-Si, the "thermal spike" model is used in order to describe the energy transferred to the amorphous film (see ref. 19 and its references). This means that the ion deposits its energy along its path through the material, resulting in a sudden temperature rise followed by a fast cooling of the material within a cylinder of a few nm. Calculations have shown that the lifetime of such a "thermal spike" is about 10^{-10}s. Considering a similar value of the heat dissipation speed, we can conclude that the "thermal spikes" of two consecutive laser shots will not overlap. In order to calculate the macroscopic temperature of the sample during the laser irradiation the associated heat equation must be solved. However, for this work we will only note the anisotropy of the problem.

3.3 Investigations methods

The signature of the material structure at atomic level is generally found in the IR vibrational spectra and X-ray photoluminescence spectra (XPS). The first measurement technique reveals the atomic bonds investigating the material bulk, while the second provides information from the surface (the depth penetration in XPS measurements is 3 nm estimated). For this study, the IR measurements were carried out in the absorption mode using a FTIR spectrophotometer with 4 cm^{-1} resolution in the range 550 – 4000 cm^{-1}.

Special attention was paid to the IR absorption peak placed around 1000 cm^{-1} and assigned to the stretching vibration mode. Studying a series of SiO_x with $0<x<2$ by IR spectroscopy, a calibration curve that relates the peak position corresponding to this vibration with the x parameter can be build up. Such a calibration is utilised to identify the layer composition from IR measurements.

The Si-Si vibrations are revealed by Raman spectroscopy which relies on inelastic scattering of monochromatic light, usually from a laser. The laser photons interact with phonons or other excitations in the system. The energy of the scattered photons, if the vibration modes are Raman active, is shifted up or down. This shift gives information about the phonon modes in the system. Infrared spectroscopy yields similar, but complementary, information. In this study the Raman measurements have been made with a system formed from a LabRam from Jobin Yvon analyzer integrated with an Olympus BX40 microscope.

The XPS measurements have been made with a Vacuum Generators XR2E2 Twin Anode X-ray Source (Mg-K_α source operating at 120 W). The X-ray photons, with a well-defined energy, determine the emission of the photoelectrons from core levels of the atoms of the investigated material (SiO_x). A hemispherical analyzer CLAM-2 was used to analyse the photoelectrons' spectra. By measuring the photoelectron energies, the binding energy values of corresponding core level electrons can be determined. The selected conditions for the measurement allowed discriminating binding energies of 0.2 eV.

In order to investigate the density of the paramagnetic defects, Electron Paramagnetic Resonance (EPR) measurements were performed with a Bruker ESP 300 X-band spectrometer equipped with a rectangular cavity (TE102 mode, unloaded Q=4000). The as deposited and laser irradiated SiO_x samples have been mounted on a special teflon sample-holder and placed at the centre of the cavity. The EPR spectra were measured at room temperature and the microwave power was 1.3 10^{-3} W. The field modulation had a frequency of 100 kHz and amplitude of 3420 G. The spectrometer time constant was 41 msec, the ADC conversion time was 82 msec. The microwave frequency was around 9.43 GHz. Defects spin densities were determined by comparison with a MnO

[20] Wolfgang Theiss, Solutions for optical spectroscopy in http://www.wtheiss.com/

sample with a known spin density of $3\pm1\cdot10^{15}$ spins and located directly under the sample during EPR measurements. The procedure provides relative spin densities with an accuracy of ca. 10%.

4. Results and discussions

4.1 IR investigations

In this work, the IR investigation will focus on stretching vibration mode of the Si-O-Si bridge revealed by an asymmetric peak placed at 1000 cm^{-1}. To better visualise the changes in the peak position and peak width, all spectra have been normalised at the peak height.

In Fig. 3 are shown the IR spectra of the as deposited samples and of the laser irradiated samples with various amount of the UV photons. The peak position of the IR stretching vibration mode measured on irradiated samples is shifted towards higher wave-number values . For a better understanding, we mention the peak position for sputter[21] deposited SiO_2 at 1054 cm^{-1}. The as deposited $SiO_{1.2}$ samples are characterised by a peak position at 1027.7 cm^{-1}. After the laser irradiation, the main peak has its maximum at 1068.2 cm^{-1}, when the laser energy is 55 mJ (which means 103.4 mJ/mm^2). The full width at half-maximum (FWHM) - an indicator of the structural homogeneity – was also changed by UV irradiation. For the as deposited sample, the width of the peak was found 146.4 cm^{-1} and for the UV irradiated sample 106.1 cm^{-1} (55 mJ).

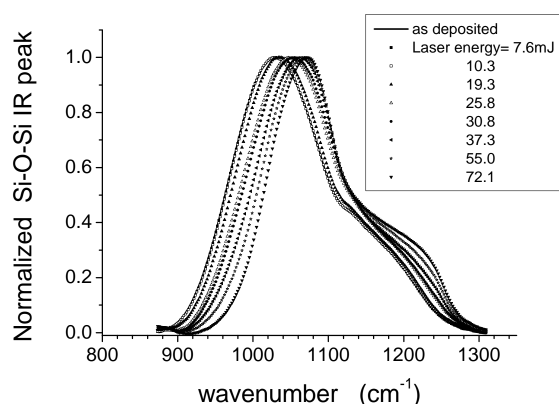

Fig. 3. The normalized IR absorption spectra of the stretching vibration mode for as deposited (full line) and UV irradiated samples with various laser energy(symbols). The energy delivered during the laser treatment is a measure of the number of the incident photons.

Other issues related to the changing of the peak shape are:

i) the IR spectra of the laser treated samples have the main peak placed nearer the peak position of the thermally growth SiO_2, 1073 cm^{-1} (red shifted in comparison with the sputter deposited SiO_2;

ii) the spectrum of the irradiated sample has a shoulder at 1250 cm^{-1} that is specific to the SiO_2 structure;

iii) the shift in the peak position is dependent on the energy transferred to the SiO_x via photon impacts.

Generally, the shift in the peak position and the changes in the peak shape show the structural changes in material. Fig. 4 reveals the shift in the peak position and its dependence on the incident photons' energy.

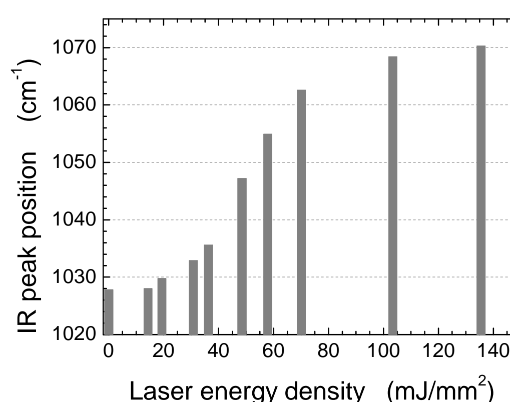

Fig. 4. The shift of the peak position assigned to the Si-O-Si stretching oscillation mode with increasing the UV photon's energy.

Supposing the same number of Si and O atoms in the structure of the as deposited sample as in that of the laser treated sample, the IR spectra show phase transformation of the material as:

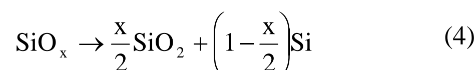

$$SiO_x \rightarrow \frac{x}{2}SiO_2 + \left(1-\frac{x}{2}\right)Si \qquad (4)$$

with intermediary steps, depending on the incident energy:

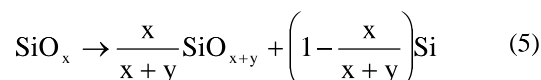

$$SiO_x \rightarrow \frac{x}{x+y}SiO_{x+y} + \left(1-\frac{x}{x+y}\right)Si \qquad (5)$$

The peak shape is drastically changed when more energy is added in the layer, especially after the corresponding value of the SiO_x dissociation energy is exceeded. Having a calibration curve IR peak position versus oxygen content for $0<x<2$, the value of the y parameter can be calculated. In this way, the formation of oxygen rich regions in SiO_x can be revealed.

For a well understanding of the IR measurements, the depth penetration of the laser photons and their absorption in SiO_x have to be considered. A sample with a larger thickness than the depth penetration (which is the case in

---

[21] N. Tomozeiu, J. J. van Hapert, E. E. van Faassen, W. Arnoldbik, A. M. Vredenberg and F. H. P. M. Habraken, J.of Optoelectronics and Advance Materials, vol 4 nr 3, 513-522, (2002)

these experiments), will have structural transformation into the layer part defined by the dept penetration. This region will have domains with higher x value (and implicitly, others with smaller x values). Also, the optical constants (refractive and absorption indexes) and the depth penetration of the laser photons will change. The latter increases with the x value. This means, increasing the laser energy into the SiO_x, the depth of penetration increases and more material will get phase separated. Such a progressive structural change is revealed by the IR spectra shown in figure 4. However, the samples here studied will have an "as deposited" material region situated under the laser treated region. That is, the spectra of the SiO_x samples irradiated with more photons reveal two peaks: one that belongs to the transformed material (its peak position increases with the laser energy) and the other one assigned to the as deposited material. According to the model above described the second contribution to the IR stretching peak decreases with increasing the laser energy. A mathematical description of the two contributions to the IR spectrum is:

$$I_k^{meas} = q * I_{as_dep} + I_k \quad (6)$$

where I_k is contribution of the laser treated region and I_{as_dep} represents the as deposited region. The sub-unitary multiplication factor q can be calculated using a fitting routine of the peak shape with two gaussians. For the samples here-studied the q-parameter values are shown in Fig. 5.

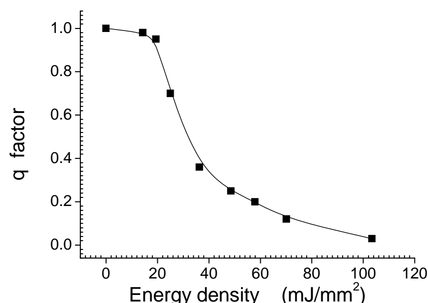

Fig. 5. The evolution of the q factor from the IR spectra fit, when the laser energy increases.

Increasing the laser energy, more and more as deposited material is phase separated. This is explained by the decrease of the q values.

4.2 Raman spectroscopy and crystalline entities

If the O-Si bonds' clustering to make highly oxygenated structural entities have been revealed by the IR spectra, what about the Si-Si bonds? For a system where the total number of silicon and oxygen atoms is conserved, increasing the number of O-Si bonds has repercussions on the number of Si-Si links.

The evolution of the Si–Si bonds number can be studied by Raman spectroscopy. For amorphous silicon the Raman signature is a wide peak centered on 480 cm^{-1}. If the material is crystalline, the Raman spectrum has a very sharp peak[22] at 520 cm^{-1}. The figure 6 shows the Raman spectra of $SiO_{1.2}$ as deposited and laser treated samples. Increasing the laser energy, the peak centered at 480 cm^{-1} increases in intensity. Qualitatively, this means that the amount of Si–Si bonds has been increased by UV photon irradiation. Therefore, the IR spectroscopy revealed the increasing of the Si-O bonds' number and the Raman investigations showed the increase of the Si-Si number when the SiO_x sample has been laser irradiated. Increasing the energy delivered to the material, more oxygen-rich and silicon-rich material has been detected.

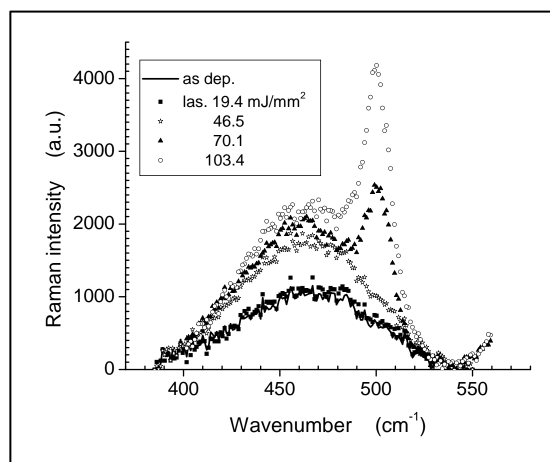

Fig. 6. The Raman spectra provide information regarding the increasing of Si-Si bonds when the photons' energy increases. The spectra of the samples irradiated with 70.1 and 103.4 mJ/mm^2 show the development of crystalline silicon from amorphous phase.

Increasing more the energy delivered to the SiO_x it is possible to induce the phase separation (silicon and SiO_2) together with the phase transformation*: from amorphous into crystalline silicon*. The sharp peak centred on 520 cm^{-1}, which is the fingerprint for crystalline silicon, increases in intensity with increasing the energy above a certain threshold value. Fitting the Raman spectrum with two gaussians – one for amorphous phase and the other for crystalline phase – the amount of the silicon transformed in crystalline silicon can be evaluated: 15.9% and 28.3% for incident UV energy of 70.1 mJ/mm^2 and 103.4 mJ/mm^2, respectively. This proves the possibilities of the method to obtain Si-nc embedded into SiO_2 matrix.

4.3 XPS spectra reveal the SiO_x structural changes

The bonding of a silicon atom to other silicon and/or oxygen atoms is well revealed by the XPS spectra: the peaks that correspond to Si (2p) and O(1s) core levels' electrons. The effect of the electronic charge transfer from Si to O in the formation of a Si-O bond appears very

[22] S. Hayashi, K. Yamamoto, J. Lumin. 70 (1996) 352.

distinctive in the Si (2p) peak shape. Due to the additional positive charge on the silicon atom, the binding energy of the Si (2p) electrons increases with more oxidised surroundings. The binding energy for Si (2p) in Si^0 configuration (a tetrahedral arrangement where a central Si atom is surrounded by other four silicon atoms) is 99.15 eV, while for a Si^{4+} configuration (the central Si atom is bonded to four oxygen atoms) it amounts to 103.4 eV[23]. In between these two extremes there are configurations as Si^{n+} where n=1, 2, 3. Each of them is characterised by a binding energy value, as it is shown in ***table 1***. With these data, every Si(2p) peak can be deconvoluted revealing the contributions of the five structural entities Si^{n+} (with n=0, 1, 2, 3 and 4).

Fig. 7 shows the XPS spectra measured on as deposited $SiO_{1.2}$ and UV irradiated samples. The shift of the main peak position towards larger values of the binding energy and the development of the low oxidised contributions (the peak around 100 eV), with increasing the photons' energy, illustrate the structural changes. The shift means more SiO_2 and the peak corresponding to 99.15 eV means more silicon in the material structure. Using the deconvolution of the XPS spectrum these observations can be quantitatively revealed. The insert from Fig. 7 shows such a deconvolution for the as deposited sample.

Fig. 7. The XPS spectra of Si (2p) electrons measured on $SiO_{1.2}$ as deposited and UV irradiated with various amounts of photons. The insert shows the deconvolution of the as deposited $SiO_{1.2}$ spectrum.

Table 1. Binding energy values of Si (2p) electrons in Si^{n+} configurations.

n (in Si^{n+})	0	1	2	3	4
Energy (eV)	99.15	100.15	100.85	101.65	103.05

[23] C. Wagner, W. Riggs, L. Davis, J. Moulder and G. Muilenberg (Ed), *Handbook of X-ray photoelectron Spectroscopy*, Perkin-Elmer Corp. Eden Prairie, Minnesota, USA, 1978

Following this procedure the Si^{n+} contributions have been calculated for all samples and they are shown in Fig. 8. The reference values for all structural entities were considered those of the as deposited status, which are: Si^0 6%, $Si^{1+}$and Si^{2+} each 5.5%, Si^{3+} is 17% and Si^{4+} about 66%. As one expected, the high-oxidised building blocks are preponderant. Increasing the laser energy, for irradiation with more than 19.3 mJ/mm^2, the contribution of Si^{2+} tetrahedra decreases. Both Si^0 and Si^{4+} configurations increase with the applied laser energy. As the figure 8 shows, these two structural entities are more and more when increasing the incident energy. Structural entities as Si^{1+} and Si^{3+} represent the interface between these two phases. It is interesting to mention that Si^{1+} increases at low energy of the incident photons up to 48.5 mJ/mm^2. For the same range of the energy, the Si^{3+} structure decreases. For higher values of the energy density, both Si^{1+} and Si^{3+} structures decreases as number. Everything goes to Si^0 and Si^{4+} clusters that increase as dimension (see the relation 4).

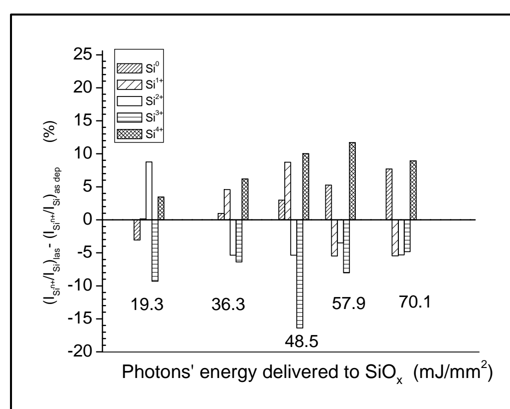

Fig. 8. The changes in the amount of Si^{n+} (n=0, 1, 2, 3, 4) entities when the sample is irradiated with various amounts of UV photons. The data are relative to the as-deposited sample. Each group of bars in the plot represents one sample irradiated with the UV photons having the energy written under the plot.

Mathematically this can be written as:

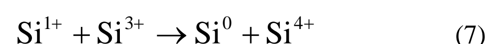

$$Si^{1+} + Si^{3+} \rightarrow Si^{0} + Si^{4+} \quad (7)$$

We note the numbers of both the silicon and the oxygen atoms remain constant in this phase separation process.

4.4 EPR measurements reveal the DB defects

The defects' density is a very important parameter for thin films of silicon suboxide because it defines the electrical properties of the layers. Elsewhere[24], it was

[24] N. Tomozeiu, E.E. van Faassen, W.M. Arnoldbik, A.M. Vredenberg, F.H.P.M. Habraken, Thin Solid Films **420 – 421** (2002) 382

shown that for SiO_x are characteristics the dangling bonds (DB) defects of silicon and the so-called E' defects specific to SiO_2 structures. In this work we focus on paramagnetic DBs that are neutral defects D^0. For this it was used the Electron Paramagnetic Resonance (EPR) technique, where the D^0 system of electrons interacts with an external magnetic field, the SiO_x sample being exposed to microwaves at a fixed frequency. When the gap in energy between the two spin states assigned to D^0 matches the energy of the microwaves, there is a net absorption of energy that can be converted into a spectrum.

Generally, the derivative absorption of microwave power (which is the EPR signal) is measured as a function of the magnitude of an externally applied magnetic field, B. The coupling of the electromagnetic field (microwave range) with the D^0 system is characterized by a resonant frequency f=g·B, where g is the Landee' factor. The value of the g parameter is the fingerprint for the defect type. In literature, g =2.0055 is assigned to a-Si dangling bond defects (DB), while g = 2.0012 is due to E' defects from SiO_2. The as deposited $SiO_{1.2}$ had a g value of 2.0035, which is assigned to the DB a-Si defects surrounded by oxidized neighbours.

The double integral (DI) of the EPR signal is proportional to the number of oscillators (defects). Considering the area of the UV irradiated surface (26.6 mm^2), the geometry of the investigated samples (the total surface area, A, of the sample) and the q factor - that shows how much $SiO_{1.2}$ material remains non-treated by the UV photos (see the figure 5) - the amount of DB a-Si defects can be calculated. In order to reveal the photons' influence on the defects' number, a parameter δ has been defined:

$$\delta = \frac{di_{irr} - q \cdot di_{as_dep}}{di_{as_dep}} \tag{7}$$

where the di_{as_dep} is the double integral of the EPR signal normalized to the irradiated area:

$$di_{as_dep} = \frac{DI_{as_dep}}{A} \cdot 26.6 \tag{8a}$$

and the di_{irr} is the value of the EPR double integral of the irradiated region

$$di_{irr} = DI_{measured} - DI^{area}_{no_irrad} \,. \tag{8b}$$

In Fig. 9, the parameter δ is plotted against the UV energy utilized to irradiate the sample. As it can be seen, increasing the number of photons, the amount of D^0 defects increases. Till now, there is no explanation for the distribution of the experimental points against the UV energy. Important to be noted is the fact that no trace of E' centers (defects specific to SiO_2 structural entities) has been detected even after high laser energy irradiation. We consider that this subject of structural defects created by energetic photons needs more investigation and it can be an interesting topic for the future research.

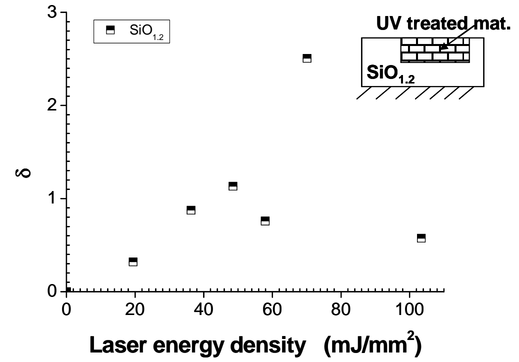

Fig. 9. The parameter δ is a measure of the paramagnetic defects, D^0 created by laser photon interacting with the SiO_x structure (see the text). This plot shows an increase of the D^0 amount with the utilized energy.

5. Conclusions

Within this work we have presented the possibility to obtain silicon nano-crystalls embedded into silicon dioxide from SiO_x treated post deposition with UV laser photons. It is already known that such new materials are very much required for silicon based light emitters in integrated optoelectronics.

It was found that:

a) regions more oxidized are formed under the interaction between the photons and SiO_x. This was revealed by IR spectroscopy, where the peak position and the shape of the Si-O-Si stretching vibration mode are changed as a function of the photons' energy (e.g. the peal-position for $SiO_{1.2}$ as deposited was 1027.7 cm^{-1} was found 1047.2 cm^{-1} for 48.5 mJ/mm^2 and 1068.4 cm^{-1} for 103.4 mJ/mm^2);

b) silicon rich material appeared after irradiation with UV photons. The Raman spectra revealed the amount of amorphous silicon that increases with the transferred energy. Moreover, increasing the photons' energy, the phase transformation from amorphous into crystalline silicon was clearly shown.

c) new Si^0 and Si^{4+} structural entities are formed in irradiated SiO_x from Si^{1+}, Si^{2+} and Si^{3+} . This was attested by XPS spectra;

d) by treating with UV photons, the number of paramagnetic dangling bond defects in $SiO_{1.2}$ increased. Qualitatively this is understood by the mismatch of the silicon lattice and the SiO_2 lattice; the intermediate phases as Si^{1+} and Si^{3+} made the transition between the two stable phases (Si^0 and Si^{4+}). However, in order to be utilized as material for optoelectronic devices, this new functional SiO_x material needs more investigations.